The horizontal scale of rotating convection in the geostrophic regime

By SATOSHI SAKAI

School of Earth Sciences, IHS, Kyoto University, Kyoto 606-01, Japan

The horizontal scale of rotating convection with rigid boundary conditions is studied. The range of Rayleigh number concerned is moderate, i.e. large enough to induce a finite-amplitude convection but small enough so that the geostrophic processes are significant.

On considering an experimental law of the Nusselt number and some constraints of elemental geostrophic processes, the horizontal scale of the convection can be estimated. This estimation strongly depends on the ratio between the thicknesses of the Ekman layer and the thermal boundary layer, and does not depend monotonically on the Rayleigh number. This dependency is compatible with the experimental results of Rossby (1969).

The estimated horizontal scale was checked by laboratory experiments. The horizontal temperature distribution was visualized by thermal liquid-crystal capsules dispersed in the working fluid. The horizontal scale was measured by counting vortices. The experimental results agree fairly well with the estimated scale.

1. Introduction

Recently a number of experimental studies (Fernando, Chen & Boyer 1991; Jones & Marshall 1993; Maxworthy & Narimousa 1994; Klinger & Marshall 1995) have been carried out on rotating turbulent convection. In these studies, experiments were done at high Rayleigh numbers so that the results could be compared with geophysical flows such as deep ocean convection. The dynamics at high Rayleigh numbers, however, were very complicated and difficult to understand. Even in the range of moderate Rayleigh numbers and Taylor numbers, we know very little about rotating convection other than the critical curve and critical mode.

Rotating convection was first studied by Jeffereys (1928), but since then only a few studies had been done until recent studies of turbulent convection. Chandrasekhar (1953) obtained the stability curve and the horizontal scale of the critical mode for stress-free boundaries and rigid boundaries, using a linear theory. It gives the critical Rayleigh number as

$$Ra_c \sim 8.7 \times Ta^{2/3}, \tag{1.1}$$

for sufficiently large Taylor numbers. This critical curve was checked experimentally by Nakagawa & Frenzen (1955).

Rossby (1969) performed extensive laboratory experiments at relatively low Rayleigh numbers and low Taylor numbers with rigid boundary conditions for water, silicone oil and mercury. He obtained horizontal scales of the convection in silicone oil, which showed a maximum value at a Rayleigh number larger than the critical value by an

order. He also obtained Nusselt numbers for the rotating convection. Boubnov & Golitsyn (1986) performed many experiments for distilled water with a free surface, at a different parameter range. They measured the horizontal scale of the convection by counting the number of vortices, and found an empirical law for the scale, which shows a monotonic dependency on the parameters.

These experiments were done in a range of moderate values of parameters just above the critical Rayleigh numbers, which are large enough to induce finite-amplitude convection, but small enough that the geostrophic processes are significant. In these conditions, the convective flows are more reproducible than the recent studies of turbulent convection, and therefore, theoretical approaches are expected to be easier. Even in this range, however, we have insufficient knowledge to understand the dynamics. For example, the experimental information we have are two different experimental results (Rossby 1969; Boubnov & Golitsyn 1986) for different boundary condition at different parameters, and we have no theoretical prediction for the horizontal scale.

The present study deals with rotating convection in a parameter range studied by Boubnov & Golitsyn (1986), and with a rigid-lid boundary condition similar to Rossby (1969) to complement these studies. A theoretical estimation of the horizontal scale of the convection for the rigid boundary condition is presented in the next section. Although it uses an empirical law for the Nusselt number, it is the first theoretical estimation for the horizontal scale of finite-amplitude convection in the rotating frame. This estimation was checked by laboratory experiments in §3. In the experiments, thermotropic liquid-crystal capsules were used to visualize the distribution of the horizontal temperature. The horizontal scale was measured by counting the number of cold or hot vortices in the fluid.

2. Theoretical estimation for the horizontal scale

Suppose a convecting layer in a rotating system is bounded by horizontal rigid plates at constant temperature. The governing non-dimensional parameters are the Rayleigh number

$$Ra = \frac{\alpha g \Delta T H^3}{\nu \kappa}, \tag{2.1}$$

and the Taylor number

$$Ta = \frac{f^2 H^4}{\nu^2}, \tag{2.2}$$

where α is the thermal expansion coefficient of the fluid, g the gravitational acceleration, f the Coriolis parameter, ΔT the temperature difference between the top and bottom boundaries, H the depth of the fluid, and ν and κ are the kinematic viscosity and the thermodiffusivity, respectively.

When the Rayleigh number is large enough to induce a finite-amplitude convection, and small enough so that the effect of rotation is significant, up-welling and down-welling of the rotating convection are restricted to narrow columns, as pointed out by Boubnov & Golitsyn (1986), because the rotation of the fluid tends to inhibit the convective motion. The rest of the interior region is expected to be in geostrophic balance. This structure can be seen also in the experiments by Nakagawa & Frenzen (1955). Such a convective regime is called the geostrophic regime hereafter. Considering the symmetry of the boundary conditions, the geostrophic vortices around the columns should circulate in opposite directions in the upper and lower parts. The up-welling and down-welling flow should be connected horizontally at the top
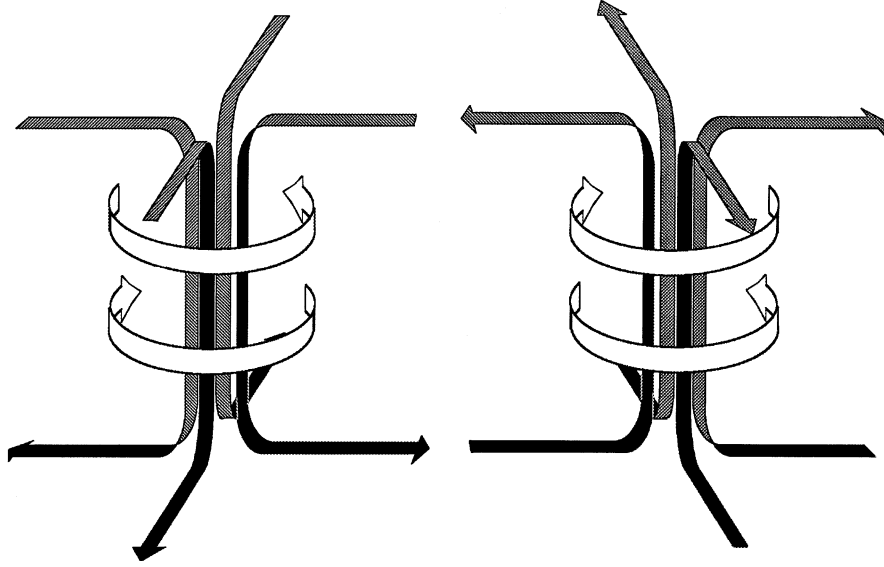
FIGURE 1. Schematic figure of rotating convection in the geostrophic regime. Narrow columns of up-welling and down-welling are enclosed by geostrophic circulation.

and bottom boundary layers to form closed cells as shown in figure 1. Based on this structure we can estimate the horizontal scale of the convection from some constraints due to elemental processes, as follows.

Suppose the temperatures of the hot and cold columns are vertically uniform and differ by ΔT_c, and these columns are separated by a distance L. Assuming the geostrophic balance in the interior region, we can obtain the typical geostrophic velocity V_0 at the upper or lower part of the interior region by vertical integration of the geostrophic equation,

$$V_0 = \frac{\alpha g \Delta T_c H}{2fL} \tag{2.3a}$$

$$= \frac{\kappa}{2L} \left(\frac{\Delta T_c}{\Delta T} \right) Ra Ta^{-1/2}. \tag{2.3b}$$

Assuming a checker-board pattern in the up-welling and the down-welling regions, the Ekman transport Q which flows into the columns is estimated at

$$Q = 4L \frac{V_0 \delta_e}{2} \tag{2.4a}$$

$$= \sqrt{2}\kappa H \left(\frac{\Delta T_c}{\Delta T} \right) Ra Ta^{-3/4}, \tag{2.4b}$$

where

$$\delta_e \equiv \left(\frac{2\nu}{f} \right)^{1/2} = \sqrt{2}H Ta^{-1/4}. \tag{2.5}$$

The temperature difference between up-welling and down-welling columns, ΔT_c, is not necessarily equal to the imposed temperature difference ΔT, because the temperature in the Ekman layer is not uniform. If we assume that the temperature is well mixed when the Ekman transport turns into the vertical columns, it can be

estimated by the weighted average of the temperature in the Ekman layer. Assuming an exponential profile of the temperature in the thermal boundary layer, we get

$$\frac{\Delta T_c}{\Delta T} = \frac{\int_0^\infty (T - T_0)v_e \mathrm{d}z}{\int_0^\infty v_e \mathrm{d}z} \qquad (2.6a)$$

$$= \frac{\int_0^\infty \exp(-z/\delta_t)\exp(-z/\delta_e)\sin(z/\delta_e)\mathrm{d}z}{\int_0^\infty \exp(-z/\delta_e)\sin(z/\delta_e)\mathrm{d}z} \qquad (2.6b)$$

$$= \frac{\int_0^\infty \exp(-\eta/D)\sin(\eta)\mathrm{d}\eta}{\int_0^\infty \exp(-\eta)\sin(\eta)\mathrm{d}\eta} \qquad (2.6c)$$

$$= 2\frac{D^2}{1 + D^2}, \qquad (2.6d)$$

where T_0 is the average temperature, v_e is the Ekman velocity towards a column, δ_t is the thickness of the thermal boundary layer, $\eta \equiv z/\delta_e$, and $D \equiv \delta_t/(\delta_e + \delta_t)$.

Obviously the vertical temperature gradient is negative in the Ekman layer, but this negative stratification is expected to have no significant effect on the dynamics of the Ekman layer because the Rayleigh number defined by thickness of the Ekman layer or thermal boundary layer is always small, and therefore small-scale convective motion in the Ekman layer is impossible.

Using (2.4) and (2.6) we can calculate the heat transport by a pair of a up-welling and down-welling columns. This heat transport should be same as that through the thermal boundary layer over the area of the pair,

$$Q\Delta T_c = 2L^2 \frac{\Delta T \kappa}{2\delta_t}. \qquad (2.7)$$

To estimate the right-hand side of (2.7), we have to know the thickness of the thermal boundary layer δ_t. Rossby (1969) showed that the Nusselt number of the rotating convection is independent of the Taylor number except near the critical curve. The Nusselt number dependence of the non-rotating convection has been measured experimentally to vary as $Ra^{1/3}$, which indicates that the thickness of the thermal boundary layer is independent of the total depth of the fluid. Considering these experimental results, the thickness of the thermal boundary layer is assumed to be

$$\delta_t = 3.8HRa^{-1/3}, \qquad (2.8)$$

where the constant is chosen from Rossby (1969).

Substituting (2.4), (2.6) and (2.8) into (2.7), we get

$$\frac{L}{H} = 2.3\left(\frac{\Delta T_c}{\Delta T}\right)Ra^{1/3}Ta^{-3/8} \qquad (2.9a)$$

$$= 4.6\frac{D^2}{1 + D^2}Ra^{1/3}Ta^{-3/8}. \qquad (2.9b)$$

Figure 2 shows the horizontal scale given by (2.9). It is clear that the normalized
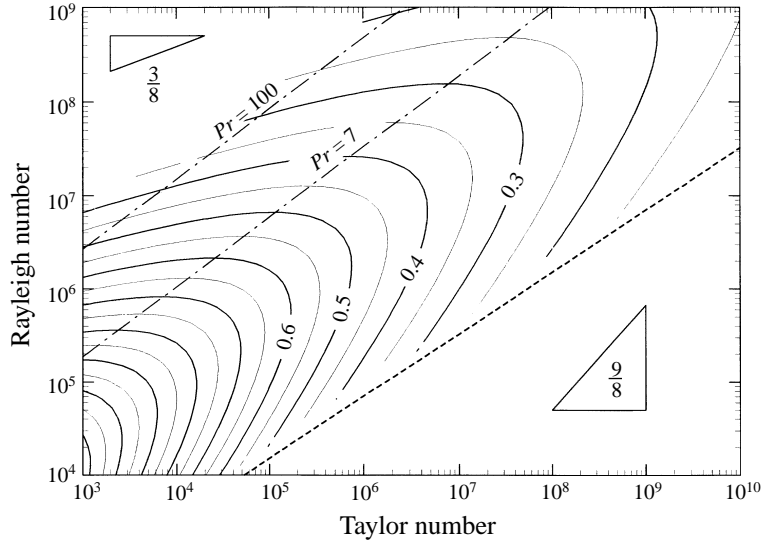
FIGURE 2. Normalized horizontal scale (L/H) of rotating convection. The dotted line indicates critical stability curve. Dot-dash-lines are the transition curves with $Ro = 1$ for $Pr = 7$ (water) and $Pr = 100$.

horizontal scale (L/H) does not depend monotonically on the Rayleigh number, but has a maximum value along the critical line. This is due to the strong dependency of D on Ta and Ra. While D is almost constant near the critical line, it approaches $D \sim \delta_t/\delta_e = 2.7Ta^{1/4}Ra^{-1/3}$ when $Ra \gg Ta$. This totally changes the dependency of the horizontal scale on Ra and Ta to

$$\frac{L}{H} \sim 33Ra^{-1/3}Ta^{1/8}, \qquad (2.10)$$

for $Ra \gg Ta$. Slopes corresponding to contour lines for $Ra^{1/3}Ta^{-3/8}$ (D =const.) and for (2.10) are also shown in figure 2.

This dependency of the horizontal scale can be physically interpreted as follows. As the Rayleigh number increases, the thermal boundary layer becomes thinner and the 'effective temperature difference' ΔT_c is reduced. (Note that the fluid in the interior region feels only ΔT_c rather than the imposed temperature ΔT.) This effect also weakens the volume flux Q given by (2.4b) and, therefore, the heat transport by a unit convective cell (left-hand side of (2.7)) is reduced. To transport heat flux given by the thermal boundary layer, the horizontal scale of the convective cells (L) must be reduced to increase the total number of cells.

The maximum of the horizontal scale is also seen in the experiments with silicone oil by Rossby (1969). Although his experiments were done with low Taylor numbers where the Ekman layers occupy the whole fluid layer while (2.9) can be applied at higher Taylor numbers, the present results seem to be consistent with his results.

Since the discussion above is mainly based on the linear theory of geostrophic flow, we should check the self-consistency of the discussion by checking the nonlinearity of the flow. A possible measure of the nonlinearity is the Rossby number, the importance of which was pointed out by Griffiths (1987). He defined it as an external parameter, but for the present purpose, it is appropriate to define it as an internal parameter using the predicted velocity and scale, because we want to know the nonlinearity of the predicted flow field.

Using the typical horizontal velocity (2.3) and the horizontal scale (2.9), the Rossby number can be determined as follows:

$$Ro \equiv \frac{V_0}{fL} \qquad (2.11a)$$

$$= 4.7 \times 10^{-2} Pr^{-1} Ra^{1/3} Ta^{-1/4} \frac{1 + D^2}{D^2}, \qquad (2.11b)$$

where Pr is the Prandtl number. Again for $Ra \gg Ta$, (2.11) reduces to

$$Ro \sim 6.5 \times 10^{-3} Pr^{-1} Ra Ta^{-3/4}. \qquad (2.12)$$

The critical lines defined by $Ro = 1$ for some Prandtl numbers are also shown in figure 2. The present study concerns the flow under these lines ($Ro < 1$).

Because the length scale L used in the Rossby number is the average scale of the convection, nonlinearity of some small-scale dynamics may emerge at smaller Rossby numbers. For example, in the convective column at the centre of convection, it is natural that some nonlinear aspects are significant even when $Ro \ll 1$, because the scale of the column is small and both the horizontal and vertical velocities are maximum. The present theory, however, relies on the dynamics of the interior region, which has the scale of L, and the dynamics of the boundary layers, and it does not depend on the dynamics of the small-scale columns. Therefore, the Rossby number defined here should be a good indicator of the nonlinearity of the convection as a whole.

3. Experiment

Laboratory experiments were done using an apparatus shown schematically in figure 3. The apparatus consisted of nested boxes so that the depth of the working fluid was easily varied by changing the middle part of the box. Three boxes were used to give different depths of working fluid: 3, 6 and 9 cm respectively. The horizontal dimension of the working fluid was 20 cm × 20 cm. The boxes were made of transparent acrylic resin except for the top and bottom boundaries. Pyrex glass, 1 mm in thickness, was used for these boundaries to minimize heat loss. The temperatures at the top and bottom boundaries were kept constant by chilled and hot water, respectively. This apparatus was mounted on a rotating table 50 cm in diameter. Electric power was supplied to the rotating system through slip rings, and the chilled and hot water were circulated and controlled on the rotating table.

Distilled water is used for the working fluid in all cases to ensure the clarity of the fluid for visualization. Small amounts of thermotropic liquid-crystal capsules (about 50 μm in diameter) were dispersed for visualization. This liquid crystal changes colour from red to blue for temperature difference of about 2 °C. This colour, however, is very sensitive to the viewing angle relative to the incoming light. Therefore, it is used only for the visualization of temperature pattern, not for quantitative measurements. A sheet of light was shone into the working fluid and the two-dimensional temperature distribution was visualized. The visualized image was recorded by a video camera mounted on the rotating table. This image was also transmitted to a television monitor in the laboratory and seen in real time to confirm that the statistical steady state had been achieved.

Although the temperatures of the hot and chilled water were controlled, the heat losses at the top and bottom boundaries were not negligible, i.e. the temperature difference that was given to the working fluid (ΔT) depended on to the heat flux
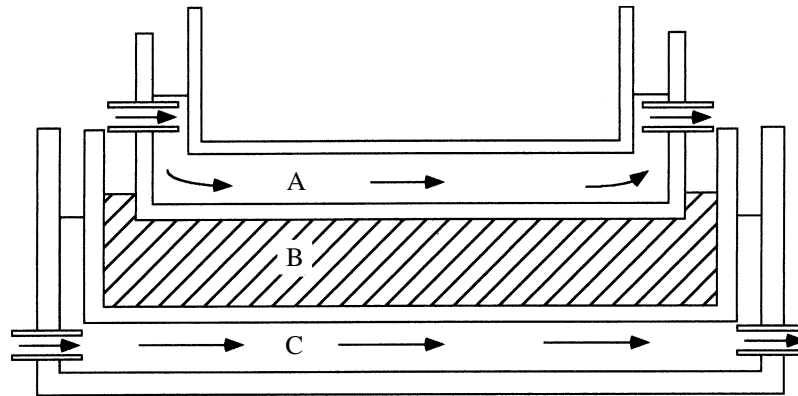
FIGURE 3. Schematic figure of apparatus. Working fluid (B) is cooled at the top by circulated chilled water (A) and heated at the bottom by circulated hot water (C).
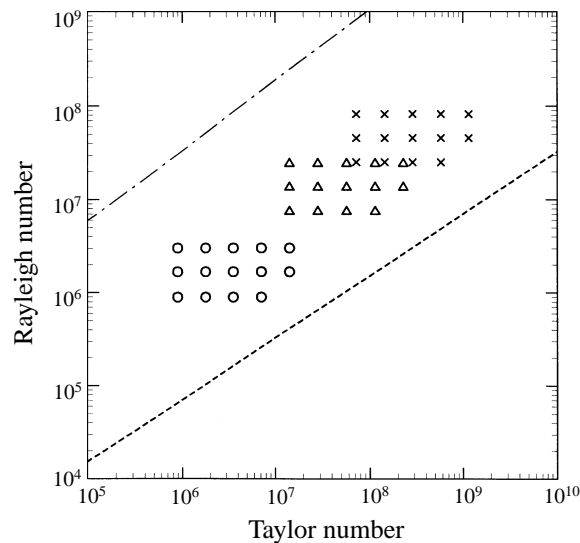

FIGURE 4. Parameters of experiments: ○, $H = 3$ cm; △, $H = 6$ cm ; ×, $H = 9$ cm. Dotted line indicates critical stability curve. Dot-dash-line is the transition curve with $Ro = 1$ for water.

through the convective layer. To correct for the temperature difference ΔT, the heat flux through the boundary was estimated by assuming the Nusselt number to be

$$Nu = 0.13Ra^{1/3}. \tag{3.1}$$

This assumption is consistent with (2.8).

Because Ra in (3.1) contains ΔT which is subject to correction, the corrective processes were taken iteratively. The corrected temperature difference ΔT ranged from 2.6 °C to 8.5 °C. The rotation speed was from 5 to 20 r.p.m. The corrected non-dimensional parameters of the experiments are shown in figure 4. Unfortunately, the parameter range of these experiments did not extend beyond the maximum of the horizontal scale (cf. figure 2), because the rotating table did not operate stably at low rotation rates.

Figure 5 shows top and side views of the typical image of rotating convection.
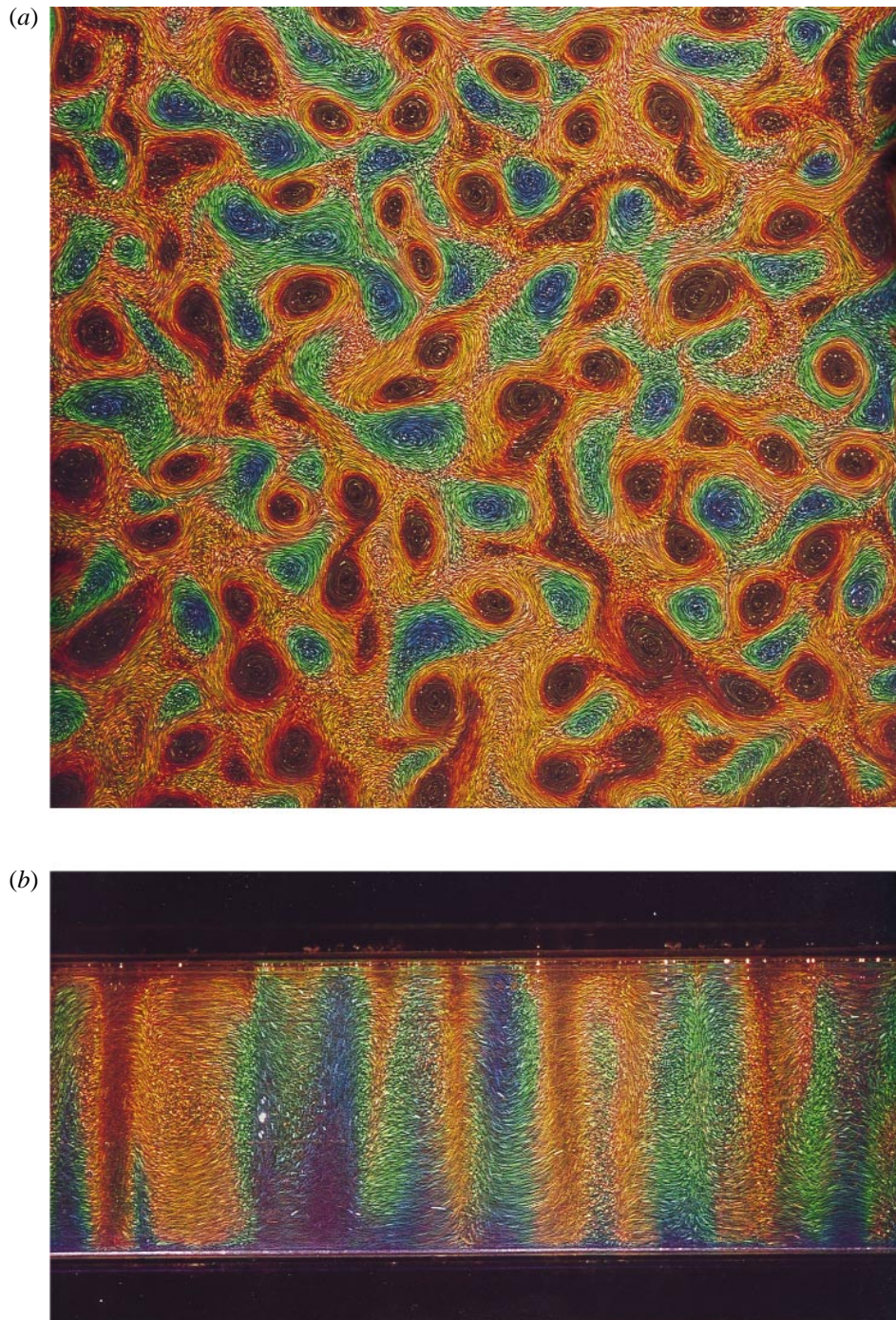
(*a*)

(*b*)

FIGURE 5. Top view (*a*) and side view (*b*) of the rotating convection for $H = 6$ cm, $\Delta T = 2.6\,^\circ$C, 14.3 r.p.m. The light sheet for (*a*) was shone at 10 mm under the top boundary.
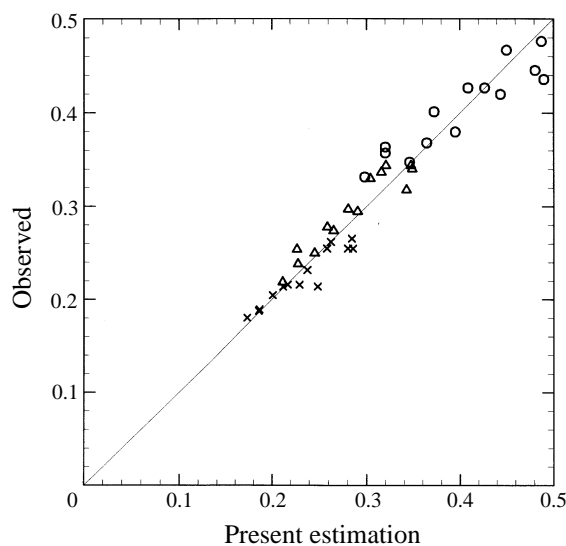
FIGURE 6. Observed horizontal scale (3.2) *vs.* estimated scale (2.9). The scales are normalized by the total depth H. The symbols are the same as in figure 4.

Regions of high temperature are shown in blue and low temperature in red. In (*a*), many up-welling and down-welling columns can be clearly seen. By changing the level of the light sheet, it was confirmed that each up-welling or down-welling column was enclosed by geostrophic vortices rotating in opposite directions at the upper and lower levels, as in figure 1. It is clear from figure 5(*b*) that the vertical temperature distribution is almost uniform.

In all cases, the columns were continuously moving around each other and no steady state, in a strict sense, was observed.

By counting the number of descending columns (N), the average horizontal scale was calculated by

$$\frac{L}{H} = \frac{L_0}{H(2N)^{1/2}} \tag{3.2}$$

where L_0 is the horizontal scale of the observed area. Figure 6 shows the observed horizontal scale and that estimated by (2.9). The experimental result agrees fairly well with the estimated one.

From streak lines in figure 5(*a*), typical horizontal velocities at the observed level are measured at 1–2 mm s^{-1}. This agrees with the geostrophic velocity estimated by (2.3) at this level ($\frac{2}{3}V_0 = 1.3$ mm s^{-1}). Figure 5(*b*) shows that the vertical velocities are observed to be of same order of magnitude as the horizontal velocity. This relatively strong vertical velocity is necessary for the narrow vertical columns to connect the top and bottom Ekman layers. In these columns, the flow cannot be geostrophic, but this does not affect the discussion in the previous section.

4. Discussion

There are some previous studies that have obtained horizontal scales which might be compared with the present result.

Chandrasekhar (1953) obtained a horizontal scale of rotating convection proportional to $Ta^{-1/6}$ using the linear theory. This horizontal scale, however, is for the
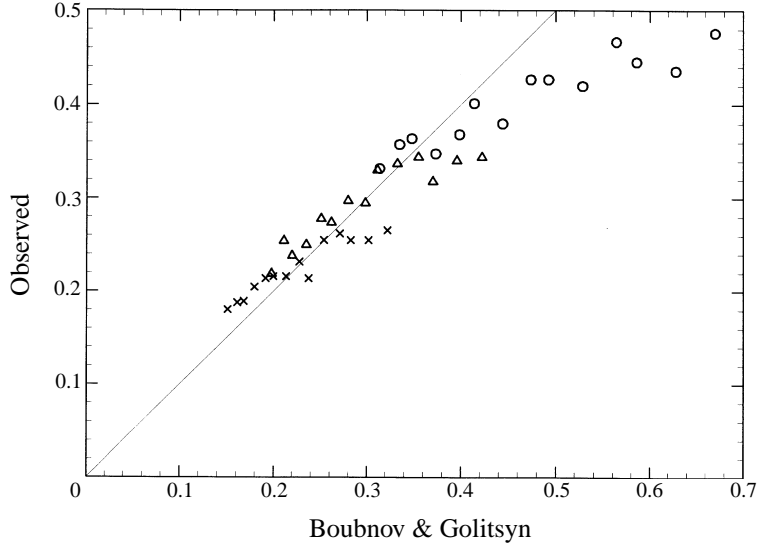
FIGURE 7. Observed horizontal scale (3.2) *vs.* Boubnov & Golitsyn's empirical law. The scales are normalized by the total depth H. The symbols are the same as in figure 4.

critical mode, and not applicable for a wide range of parameters. On the other hand, the present estimation (2.9) is not applicable for parameters near the critical curve because the Nusselt number abruptly changes there, and (2.8) cannot be applied. Therefore, (2.9) does not yield $Ta^{-1/6}$ when the critical Rayleigh number (1.1) is substituted.

Boubnov & Golitsyn (1986) found that the horizontal scale is proportional to $Ra^{1/9}Ta^{-1/4}$ in the present notation of the Rayleigh number. This empirical law is compared with the present experimental result in figure 7. Their empirical law does not match well with the present results, especially at low Taylor numbers. A possible reason is that their law was for convection with a free surface and present estimation is for two rigid boundaries. Since the present estimation strongly depends on the thickness of the boundary layers, the horizontal scale for the free surface might be controlled by different dynamics. Because the present theory is based on the convective structure consisting of the vertical columns and the horizontal Ekman layer, it cannot be applied to convection with a free surface. It is difficult to close the dynamical system only with linear geostrophic processes when the surface Ekman layer does not exist.

Maxworthy & Narimousa (1994) obtained the horizontal scale of quasi-two-dimensional vortices under the three-dimensional turbulent layer as

$$\frac{D}{H} \propto (Ro^*)^{1/2} \tag{4.1}$$

where D is the diameter of vortices and Ro^* is a natural Rossby number based on the buoyancy flux B_0. The natural Rossby number can be written in the present notation as

$$Ro^* \equiv \left(\frac{B_0}{H^2 f^3}\right)^{1/2} \tag{4.2a}$$

$$\propto Pr^{-1}Ra^{2/3}Ta^{-3/4}, \tag{4.2b}$$

where (3.1) is used to convert the buoyancy flux. Substituting (4.2) into (4.1), we get

$$\frac{D}{H} \propto Pr^{-1/2} Ra^{1/3} Ta^{-3/8}. \qquad (4.3)$$

Although the dynamics considered in Maxworthy & and Narimousa (1994) is very different from the present one, (4.3) gives very similar form to (2.9) in the present theory.

5. Concluding remarks

The horizontal scale of rotating convection in the geostrophic regime with rigid boundaries is studied. From the structure of the rotating convection, the horizontal scale was estimated using some constraints of elemental processes and an experimental law for the Nusselt number. This estimation strongly depends on the ratio between the thicknesses of the Ekman layer and thermal boundary layer, and does not depend monotonically on the Rayleigh number. This seems to be consistent with the experimental results of Rossby (1969), at low Taylor numbers.

Laboratory experiments on a rotating table were done for three different depths of working fluid. The horizontal temperature distribution was visualized by thermotropic liquid-crystal capsules dispersed in the working fluid. By counting the number of vortices in the working fluid, the horizontal scale of the convection was measured. Although the parameter range of the experiment was rather limited, the results agree fairly well with the present estimation.

Considering the strong dependency of the horizontal scale on the ratio of the Ekman layer to the thermal boundary layer, the present results might not be applicable to convection with a free surface where the surface Ekman layer does not exist.

REFERENCES

BOUBNOV, B. M. & GOLITSYN, G. S. 1986 Experimental study of convective structures in rotating fluids. *J. Fluid Mech.* **167**, 503–531.

CHANDRASEKHAR, S. 1953 The instability of a layer of fluid heated below and subject to Coriolis forces. *Proc. R. Soc. Lond.* A **217**, 306–327.

FERNANDO, H. J. S., CHEN, R. & BOYER, D. L. 1991 Effects of rotation on convective turbulence. *J. Fluid. Mech.* **228**, 513–547.

GRIFFITHS, R. W. 1987 Effects of Earth's rotation on convection in magma chambers. *Earth Planet. Sci. Lett.* **85**, 525–536.

JEFFREYS, H. 1928 Some cases of instability in fluid motion. *Proc. R. Soc. Lond.* A **118**, 195–208.

JONES, H. & MARSHALL, J. 1993 Convection with rotation in a neutral ocean; a study of open-ocean deep convection. *J. Phys. Oceanogr.* **23**, 1009–1039.

KLINGER, B. A. & MARSHALL, J. 1995 Regimes and scaling laws for rotating deep convection in the ocean. *Dyn. Atmos. Ocean* **21**, 227–256.

MAXWORTHY, T. & NARIMOUSA, S. 1994 Unsteady, turbulent convection into a homogeneous, rotating fluid. *J. Phys. Oceanogr.* **24**, 865–887.

NAKAGAWA, Y. & FRENZEN, P. 1955 A theoretical and experimental study of cellular convection in rotating fluids. *Tellus* **7**, 1–21.

ROSSBY, H. T. 1969 A study of Bénard convection with and without rotation. *J. Fluid. Mech.* **36**, 309–335.